

KRYSTYNA GADZINOWSKA, EWA PIORKOWSKA

Centre of Molecular and Macromolecular Studies  
Polish Academy of Sciences  
ul. Sienkiewicza 112, 90-363 Łódź  
e-mail: epiorkow@bilbo.cbmm.lodz.pl

## Spherulite nucleation density from thin sections of bulk samples

**Summary** — The determination of bulk spherulite nucleation density from micrographs of thin random sections is discussed. The influence of the time dependence of nucleation on average number of spherulites in a volume unit of a polymer, determined from thin sections, is estimated based on the computer simulation of spherulitic crystallization. The relevance of the proposed method is verified experimentally. The average number of spherulites in commercial isotactic polypropylenes and in nanocomposites of isotactic polypropylene with montmorillonite with bimodal nucleation are calculated. The results allow to estimate better the nucleation effect of montmorillonite on crystallization of nanocomposites.

**Key words:** isotactic polypropylene, nanocomposites, montmorillonite, crystallization, nucleation density, computer simulation.

### DETERMINATION OF SPHERULITE NUCLEATION

Growing interest in controlling the solidification of crystallizable polymers under processing conditions resulted in numerous papers dealing with the overall crystallization kinetics using both mathematical modeling and computer simulation. However, in order to predict the spherulitic crystallization kinetics the reliable data on spherulite nucleation and growth rate are required, in addition to correct mathematical models and calculation algorithms.

The spherulite growth rate depends in static conditions on pressure, temperature and molecular characteristics of a polymer. The Hoffman theory [1] dealing with crystal growth allows to explain the growth rate dependence on temperature and to interpolate or extrapolate the growth rate data obtained experimentally, usually in a limited range of temperature or pressure. The spherulitic nucleation depends on additional factors such as thermal history of a polymer and also on the presence of foreign particles nucleating polymer crystallization. Therefore, in order to characterize the nucleation process it is necessary to study it under various conditions. There are number of methods of the determination of the nucleation of polymer crystallization, including the classic Avrami analysis of isothermal crystallization data and the Ozawa approach to nonisothermal crystallization [2, 3]. However, there are numerous factors introducing errors to such analysis. Among them there are: secondary crystallization, complicated dependence of nucleation rate on time and the influence of

sample boundaries on the crystallization kinetics, including the additional spherulite nucleation on interfaces [4, 5]. To study the nucleation, one can also analyze the positions of interspherulitic boundaries in thin films [6, 7] and in sections of bulk samples [8]. This route, similarly as the Avrami analysis, requires also the knowledge of the spherulite growth rate.

Another way, although tedious, is to follow the crystallization under a microscope, to count the arising spherulites and to recalculate their numbers per volume unit of melt. However, the average total number of spherulites per polymer volume unit after completion of crystallization can be determined more easily and can give satisfactory information about the nucleation, especially if it occurs in a short time interval at the beginning of the crystallization as it occurs in some brands of isotactic polypropylene.

Often, in order to learn about the nucleation in bulk, thin films are used. Dealing with a thin film might have some disadvantages: difficulty in reproducing complicated mechanical and thermal history of a polymer or a possibility of accidental introduction of nucleating particles onto a film surface. The nucleation of crystallization by microscope glasses is also a real danger for trustworthy measurements. Recent extreme example of the strong nucleation effect caused by the presence of microscope glasses is crystallization of nanocomposites of polypropylene with montmorillonite compatibilized by maleic anhydride grafted polypropylene [9]. In addition, when the nucleation is prolonged in time, the average total number of spherulites per volume unit of a thin

film might be significantly larger than that in polymer bulk due to a slower overall crystallization.

Characteristics of the nucleation under processing conditions might require the determination of the nucleation density directly from the bulk samples, especially when dealing with thick wall articles having complicated both thermal and mechanical history, and/or in the case when spherulites are very small.

The determination of average spherulite radius, and thus the nucleation density is also possible by small angle light scattering (SALS) or by analysis of either section or cut surfaces under a microscope (light, TEM, SEM or AFM). The first method requires respectively thin samples containing no more than several layers of spherulites of sizes not exceeding 50  $\mu\text{m}$ . Moreover, the average size obtained by SALS is in fact the fifth momentum of the spherulite size distribution because the main contribution to light scattering comes from the largest spherulites. Thus, the SALS determined average size is much greater than the actual mean spherulite size.

The disadvantage of analysis of bulk sample cross-sections is that the size of an average spherulite determined in such a way, hence also the nucleation density, deviate from the true values. Simple analysis of randomly cut set of identical spheres shows that the average radius determined from the cross-section ( $R_s$ ) equals to 0.816 of the true value,  $R$  [10]. Hence, the nucleation density ( $D_s$ ) estimated based on the radius  $R_s$ ,  $D_s = 3(4\pi R_s^3)^{-1}$ , is overestimated by 84 % with respect to the true nucleation density,  $D = 3(4\pi R^3)^{-1}$ , and  $D_s = 1.84D$ .

However, the spherulites in a sample show a size distribution and moreover, the spherulites are truncated due to impingement and deviate from a spherical shape. Recently Gadzinowska *et al.* [11], based on computer simulation data, found that the radius of an average spherulite determined from the cross-section of a real bulk sample equals to 0.756 of the actual value; the bulk nucleation density calculated directly from this value is overestimated by 130 %. The computer simulation of the spherulitic structure, however, was limited only to the simplest case of instantaneous nucleation when the interspherulitic boundaries are planar.

For the nucleation prolonged in time there is a time lag between nucleation of neighboring spherulites and the interspherulitic boundary assumes a shape of a hyperboloid. In order to find the relation between the size of an average spherulite determined from the cross-section of a bulk sample and its true value when the nucleation is prolonged during the crystallization we conducted a computer simulation of the crystallization. The influence of sample dimensionality on the mean spherulite size and the average number of spherulites per volume unit of a thin film in the case of nucleation prolonged in time is also discussed. The basic relations from the probabilistic model of spherulite structure formation developed previously [12] are used.

The simulation of the crystallization nucleated in two subsequent instantaneous processes was also conducted in order to model the nucleation process in polypropylene nanocomposites with montmorillonite described in [9].

The computer model predictions were verified by comparison with the experimental data of the nucleation density in a commercial grade isotactic polypropylene. The numbers of spherulites per volume unit of isothermally crystallized samples of different isotactic polypropylenes and also nanocomposites of polypropylene with montmorillonite clay were determined, based on the analysis of thin sections of these samples.

### COMPUTER SIMULATION

In our previous publication [11] we described the computer simulation of spherulitic structure grown from instantaneous nuclei. Coordinates of spherulites centers were generated in a cube by pseudorandom number generator. On a series of probing planes crossing the simulated sample the regular dense networks of equally spaced points were chosen. For each point of the network the closest spherulite center was determined. This spherulite occluded the considered point of the network. In this manner we determined the number of all spherulites crossing each plane, and we were able to calculate the  $R_s$  value as equal to  $(N_s\pi)^{-1/2}$ , where  $N_s$  denotes the average number of spherulites crossing an area unit of cross-section.

In the calculations conducted for the time dependent nucleation process the crystallization was simulated in a cubic sample and coordinates of potential nuclei were generated by the pseudorandom number generator as described above. The spherulites crossing several selected probing planes were identified as the spherulites occluding the network points on these planes as the first ones. The average spherulite cross-section area ( $S$ ), and  $R_s$ , were determined based on these data. The nucleation occurring at a constant rate was chosen as a model of a time dependent process. Simulated crystallization consisted of alternating nucleation and growth steps. Coordinates of a fixed number of potential nuclei were generated in each nucleation step but only those points remained as nucleation sites which were located outside of other spherulites, nucleated earlier. After each nucleation step the radii of all spherulites were increased by a small constant value. The nucleation steps were repeated until the end of crystallization when no unoccupied space was left. The nucleation rate ( $B$ ), was adjusted to obtain a similar number of spherulites per unit volume ( $N$ ), as in [11], *i.e.* about  $10^4/200^3$ .

Recently, Nowacki *et al.* [9] found that in nanocomposites prepared from isotactic polypropylene, nanoclay (organo modified montmorillonite) and maleic anhydride grafted polypropylene, the additional spherulite nucleation, rapid and intense, occurred at a late stage of

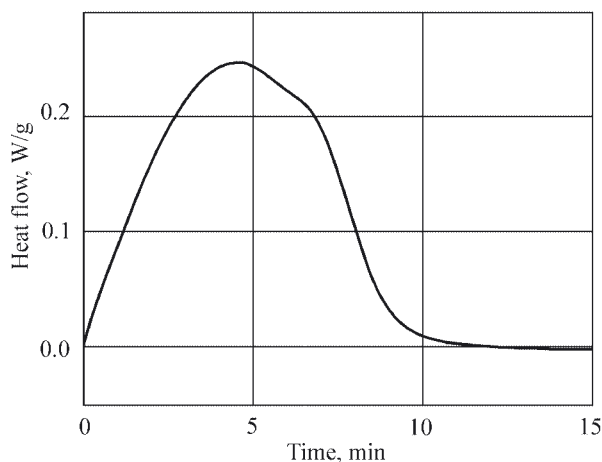


Fig. 1. DSC exotherm recorded during isothermal crystallization of compatibilized nanocomposite of Malen P F401 with 3 wt. % of montmorillonite at 128 °C [9]

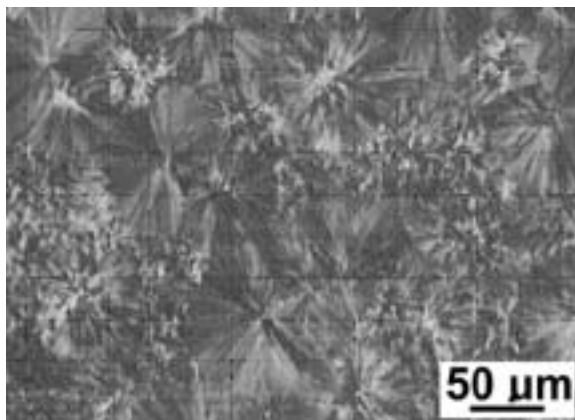


Fig. 2. Polarized light micrograph of thin section of a sample of compatibilized nanocomposite of Malen P F401 with 3 wt. % of montmorillonite, crystallized isothermally at 128 °C in DSC apparatus

isothermal crystallization, which resulted in small shoulders on the descending slopes of the DSC exotherms (Fig. 1) and in small spherulites between the large ones visible in thin sections of samples (Fig. 2). The late nucleation results from extreme sensitivity of nanocomposite to the orientational flow of the polymer melt between spherulites due to density change. In the computer simulation of such crystallization we introduced two instantaneous nucleation events: the first at the beginning of the crystallization process similarly as that used in [11], characterized by the nucleation density  $D_1$ , and, when the conversion degree reached the level of 0.75, the second one characterized by the nucleation density  $D_2$ . Only one fourth of the nuclei generated in the second step are real since the rest of them was located inside already grown spherulites, with a maximum radius ( $R_a$ ) as determined by the expression derived from the classic Avrami and Evans theory [2, 12]:

$$R_a = 3 \ln 4 (4\pi D_1)^{-1/3} \quad (1)$$

where:  $D_1$  — nucleation density of the first nucleation population, equal to  $10^4/200^3$  (i.e. 10 000 spherulite centers were generated by means of pseudorandom number generator in a cube of  $200 \times 200 \times 200$  of arbitrary units).

The calculations were conducted for a range of  $D_2$  values;  $D_2$  was usually a multiple of the density of first nucleation step —  $D_1$ . The average total  $N$  value was equal to  $D_1 + 0.25D_2$ . The volume fractions occupied by the first and the second generations of spherulites ( $V_1$  and  $V_2$ , respectively) were calculated using the rules described in ref. [12] as follows:

$$V_2 = 4\pi D_2 \int_{R_a}^{\infty} \exp\{-(4/3)\pi [D_1 r^3 + D_2 (r - R_a)^3]\} (r - R_a)^2 dr \quad (2)$$

$$V_1 = 0.75 + 4\pi D_1 \int_{R_a}^{\infty} \exp\{-(4/3)\pi [D_1 r^3 + D_2 (r - R_a)^3]\} r^2 dr \quad (3)$$

In addition, the cross-sections of simulated bulk samples were visualized. For each spherulite in subsequent short time intervals the points were calculated, where the growing spheres representing spherulites came into contact. This type of calculation was conducted for an instantaneous nucleation, a nucleation at a constant rate and bimodal instantaneous nucleation, assuming a constant growth rate of spherulites.

#### RESULTS OF COMPUTER SIMULATION

The exemplary fragments of spherulitic patterns visible in cross-sections of the computer simulated samples are shown in Fig. 3. While in the instantaneously nucleated sample (Fig. 3a) the spherulites are polygons, the cross-section of the sample with nucleation at a constant rate (Fig. 3b) reveals curved interspherulitic boundaries. The calculation of the ratio of the average spherulite radius ( $R_s$ ) determined from the cross-section to the real one ( $R$ ) defined as  $[3/(4\pi N)]^{1/3}$ , gave 0.822 for the sample with nucleation occurring at a constant rate, which was astonishingly close to the value of 0.816, calculated for a set of spheres cut at random. If the equation derived in [11] for the average number of spherulites in a unit volume ( $N$ ) [eq. (4)] is used for calculations, the

$$N = 3/4 [(R_s/R) N_s^{1/2}]^3 \pi^{1/2} \quad (4)$$

improper value of  $R_s/R$  ratio might result in an error at the level of 30 %. However, the shapes of boundaries may indicate which value of  $R_s/R$  ratio should be used.

One has also to consider that the average number of spherulites per unit volume of a polymer bulk might differ significantly from the average number of spherulites per volume unit of a thin film if the nucleation continues during crystallization. For the nucleation at a constant rate,  $N$  value and the average number of spherulites per unit area of thin film ( $N_f$ ) are described by the following equations [12]:

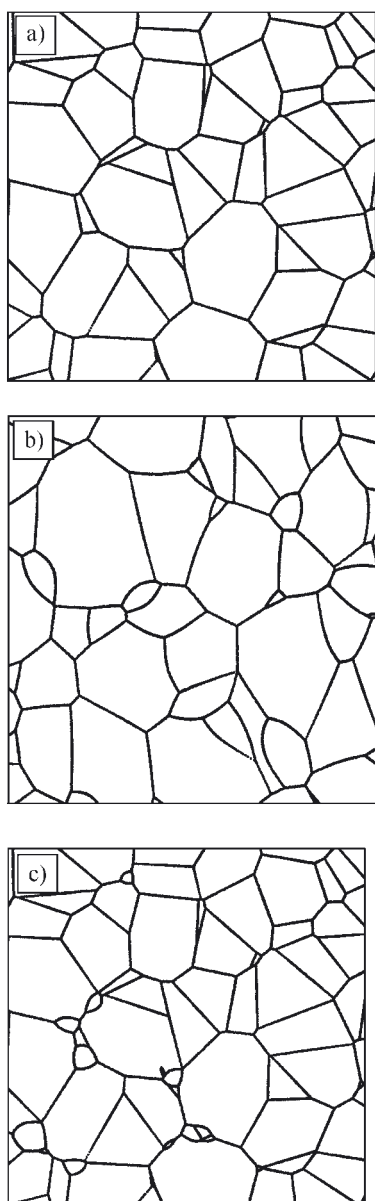


Fig. 3. Cross-sections of computer simulated samples: a) instantaneous nucleation, b) nucleation at a constant rate, c) two instantaneous nucleation events: the first at the beginning of crystallization and the second one at 75 % of conversion

$$N = (1/4) \Gamma(1/4) P^{3/4} (3/\pi)^{1/4} \quad (5)$$

$$N_f = \Gamma(1/3) P_f^{2/3} (9\pi)^{-1/3} \quad (6)$$

where:  $P$  and  $P_f$  — ratio of the nucleation rates and the growth rate, in polymer bulk and in thin film, respectively,  $\Gamma(x)$  — gamma function.

$P_f$  equals  $P \cdot d$ , where  $d$  is the film thickness, hence the number of spherulites per volume unit of the thin film ( $N_{fv}$ ) equal to  $N_f/d$ , will be:

$$N_{fv} = \Gamma(1/3) (4N)^{8/9} [3\Gamma(1/4)]^{-8/9} \pi^{-1/9} d^{-1/3} = 0.97N^{8/9} d^{-1/3} \quad (7)$$

For example for  $3 \cdot 10^3$  spherulites in a cubic millimeter of polymer bulk, the average spherulite radius equals 43  $\mu\text{m}$ . According to eq. (7),  $5.6 \cdot 10^3$  spherulites will crys-

tallize in a cubic millimeter of 10  $\mu\text{m}$  thick film of the same polymer, in which the crystallization can be treated as two-dimensional. Thus, if the influence of film thickness on microstructure is neglected, the prediction of the average number of spherulites per volume unit of polymer bulk based on the crystallization in thin films may be even more erratic than the determination from thin sections, based on eq. (4) with improper value of  $R_s/R$  ratio.

The computer simulation of crystallization with two instantaneous nucleation processes was conducted for various nucleation densities of the second process. For  $D_2$  equal to  $D_1$  the spherulites nucleated in the second process are hardly visible on cross-sections of computer simulated samples. In Figure 3c, the cross-section of spherulitic structure nucleated in two subsequent instantaneous processes is shown, the second with a density  $D_2 = 4D_1$ . On the cross-section a few additional small spherulites are visible between the large ones. Since the positions of the nuclei of the first process were the same as in the sample shown in Fig. 3a, all additional spherulites belong to the second nucleation population. It is noticed that the spherulitic pattern in Fig. 3c resembles the spherulitic structure of polypropylene/montmorillonite nanocomposite shown in the micrograph in Fig. 2. The spherulites nucleated in the second process, although their number is equal to the number of those nucleated in the first process, occupy less than 2.5 % of the sample volume as it is calculated according to eqs. (2) and (3). For the nucleation density  $D_2$  equal to  $10D_1$  the volume fraction occupied by those small spherulites reaches 4 %. As it follows from DSC thermograms of isothermal crystallization of polypropylene based nanocomposites with montmorillonite in [9], the volume fraction of those small spherulites does not exceed this value. Further increase in the nucleation density  $D_2$  led to the increase of volume fraction inhabited by those spherulites to unrealistic values.

Only a few spherulites nucleated at the late stage of crystallization are visible in cross-section in Fig. 3c, but they reduce the number average spherulite size, determined from the cross-sections, by 20 %. For the pattern shown in Fig. 3c the ratio  $R_s/R$  is smaller than the value of 0.756 found in [11], however the difference does not exceed 1.5 %. Thus, using the value of 0.756 one determines  $N$  value including the fraction of lately nucleated spherulites with the error not exceeding few percents. The increase in the value  $D_2$ , to  $10D_1$ , results, however, in the decrease of  $R_s/R$  ratio to 0.704.

## EXPERIMENTAL

### Materials

We have used in our studies four commercial grades of isotactic polypropylenes (*i*-PP). One of them was Malen P F401 ( $M_w = 3.0 \cdot 10^5$ ,  $M_w/M_n = 5.5$ , MFR = 3.0 g/10 min at 230 °C, 2.16 kg), manufactured by Orlen SA,

Poland. Other *i*-PPs were BASF (Germany) products: Novolen 1100 H ( $\overline{M}_w = 4 \cdot 10^5$ ,  $MFR = 1.8$  g/10 min), Novolen 1100 L ( $\overline{M}_w = 3.1 \cdot 10^5$ ,  $MFR = 5$  g/10 min) and Novolen 1100 N ( $\overline{M}_w = 2.5 \cdot 10^5$ ,  $MFR = 11$  g/10 min).  $\overline{M}_w/\overline{M}_n$  was equal to 5 for all three BASF *i*-PPs.

Polybond 3200 polypropylene with 1 % of maleic anhydride functional groups ( $MFR = 110$  g/10 min at 190 °C) manufactured by Uniroyal Chemical was used as a compatibilizer. Organo modified montmorillonite (MMT), Nanomer I30P, product of Nanocor, USA, was used as a filler.

### Preparation of PP samples

Malen P F401 was homogenized in a Brabender mixer. Polypropylenes of Novolen types were used as obtained, in the form of pellets. 20  $\mu\text{m}$  thick films of Malen P F401 and 300  $\mu\text{m}$  thick films of Novolen *i*-PPs were compression molded at 190 °C. The following procedure was applied for sample crystallization: films were heated to 220 °C, melt annealed for several minutes and cooled down at a rate of 10 deg/min to the isothermal crystallization temperature: 128, 132 or 135 °C and isothermally crystallized. The entire procedure was carried out under a flow of nitrogen.

### Methods

Films of Malen P F401 were placed on microscope cover glass and crystallized with free upper surface. The entire procedure was carried out in a Linkam Hot Stage mounted in a polarized light microscope. After the isothermal crystallization the sample was photographed and the number of spherulites in a large area of the film was determined. Several samples were crystallized in each crystallization temperature and analyzed. Thickness of all samples was measured and the average number of spherulites per unit volume of the film was determined.

Standard DSC specimens of diameter 5 mm were cut out of Novolen polypropylene films and crystallized in DSC apparatus, TA Instruments DSC 2920. After crystallization the samples were microtomed across the diameter to obtain 10  $\mu\text{m}$  thick sections, which were examined by light microscopy. Similarly as in the case of a thin film, the sections were photographed and the average number of spherulites per section unit area was calculated for each crystallization temperature and each material studied. Only spherulites nucleated at a distance from the edges of the samples were taken into account. Based on these data  $N$  value was calculated using eq. (4).

We have also applied eq. (4) to calculate  $N$  value in thick samples of Malen P F401, nanocomposites of Malen P F401 with MMT, compatibilized by maleic anhydride grafted polypropylene, and also in blends of Malen with the compatibilizer based on the data from [9].

The detailed description of preparation of those nanocomposites and their characterization is given in [9] and [13].

The nanocomposites containing 3, 6 or 10 wt. % of clay were prepared in a two-step process in a Brabender mixer at 200 °C: in the first step the compatibilizer was mixed with the clay in the proportion of 10:3 to obtain the concentrate, while in the second step the concentrate was mixed with the polypropylene. The blends containing 20 or 33 wt. % of Polybond 3200 in Malen P F401 were also prepared by one step blending in a Brabender mixer. In this case the concentrations of the compatibilizer were the same as in the composites. Neat Malen P F401 was also processed such way.

Approximately 300  $\mu\text{m}$  thick films were prepared from nanocomposites, isothermally crystallized in DSC apparatus, sectioned and studied by light microscopy. Reference [9] contains the detailed description of the procedure applied; which is however, identical to that described above for the samples of neat *i*-PPs.

## RESULTS AND DISCUSSION

On exemplary micrographs (Fig. 4), in thin film and in the section of the thick sample of Malen crystallized isothermally at 128 °C, the interspherulitic boundaries are mainly straight. The departure from linearity of few

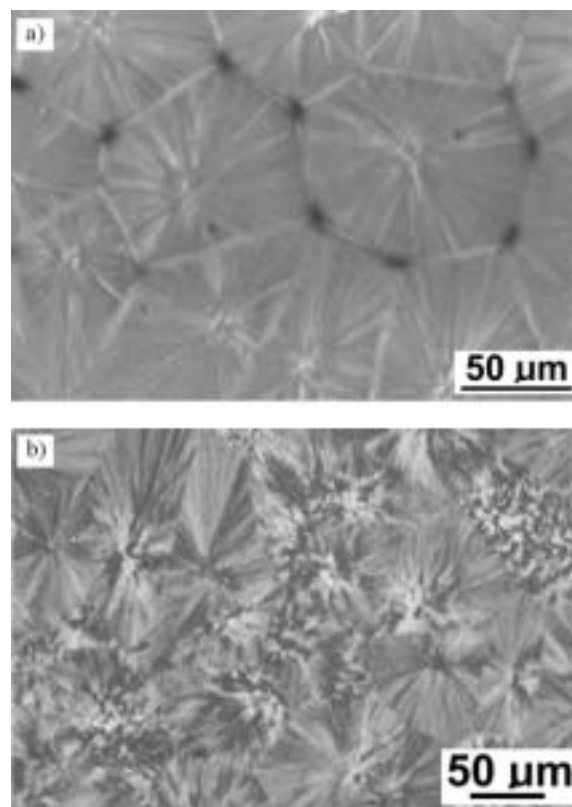


Fig. 4. Polarized light micrographs of spherulitic structure of Malen P F401 crystallized isothermally at 128 °C: a) thin film, b) thin section of a sample crystallized in DSC apparatus

curved boundaries is not very much pronounced. It indicates that the nucleation of spherulites occurs mainly at the beginning of the crystallization process. The conclusion is also supported by the direct observation of the crystallization in the thin film under the light microscope. Thus, although the dimensionality of crystallization influences the time dependence of conversion of melt into spherulites, it shows a little effect on number of nuclei per unit volume of the polymer. Since the nucleation occurs at the beginning of crystallization, the ratio  $R_s/R$  equal to 0.756 was used for the calculations based on eq. (4). The average number of the spherulites in a volume unit of the polymer in a thin film and in a thick sample crystallized isothermally, plotted as a functions of crystallization temperature in Fig. 5, are in good agreement.

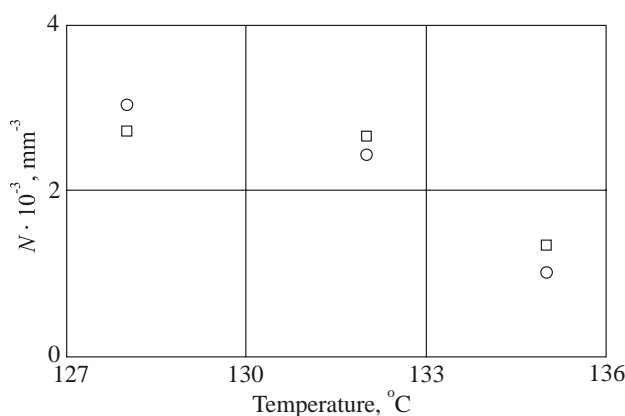


Fig. 5. Average number of spherulites per volume unit of Malen P F401 versus isothermal crystallization temperature determined (128, 130 or 135 °C): (○) thin section of DSC sample, (□) thin film

In Figure 6 the micrographs of microstructure of three Novolen types crystallized at 132 °C are shown. Similarly as in the case of Malen we concluded from the microscope examination of sections that the nucleation process occurs mainly at the beginning of crystallization and therefore the value  $R_s/R$  equal to 0.756 was used to calculate the average number of spherulites in a volume unit. In Figure 7  $N$  value is plotted versus crystallization temperature for all those three *i*-PPs. In all Novolen polymers the spherulite nucleation is stronger than in Malen. The most intense nucleation occurs in Novolen *i*-PP of the highest molecular weight.

Figure 8 demonstrates  $N$  value in compatibilized nanocomposites of Malen with MMT and its blends with compatibilizer, calculated based on the data from [9] and eq. (4). Since the additional nucleation process has a limited influence on  $R_s/R$  ratio, again the value of 0.756, as in the case of the neat *i*-PPs, was used for calculations.

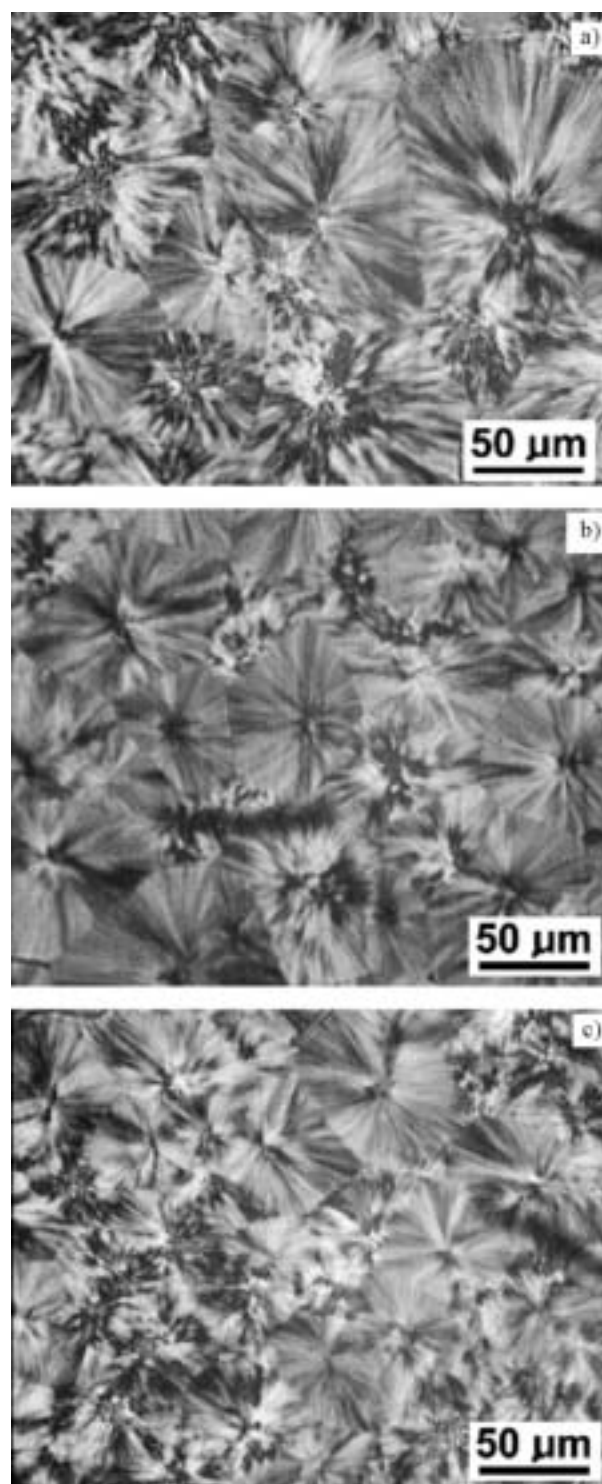


Fig. 6. Polarized light micrographs of thin sections of polypropylene samples crystallized isothermally at 132 °C in DSC apparatus: a) Novolen 1100 N, b) Novolen 1100 L, c) Novolen 1100 H

Comparison of the results obtained for nanocomposites with those for respective blends of *i*-PP with the compatibilizer indicates many folds increase in the number of spherulites per volume unit in the first case. However, the numbers in Fig. 8 are comparable with the

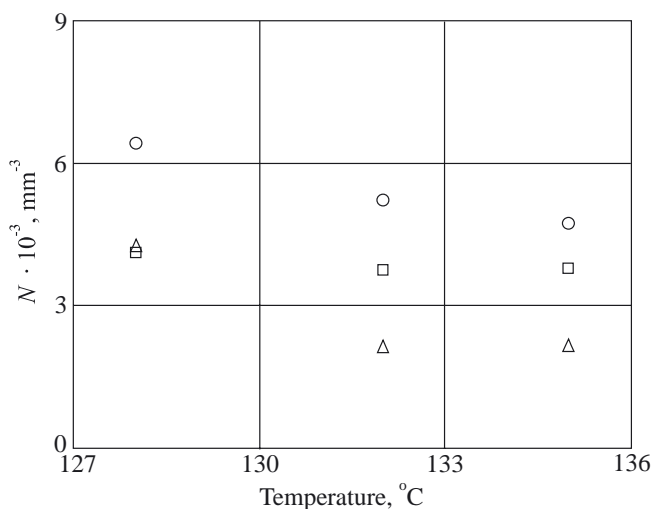


Fig. 7. Average number of spherulites per volume unit ( $N$ ) of DSC sample versus crystallization temperature, determined for polypropylenes: (Δ) Novolen 1100 N, (□) Novolen 1100 L and (○) Novolen H

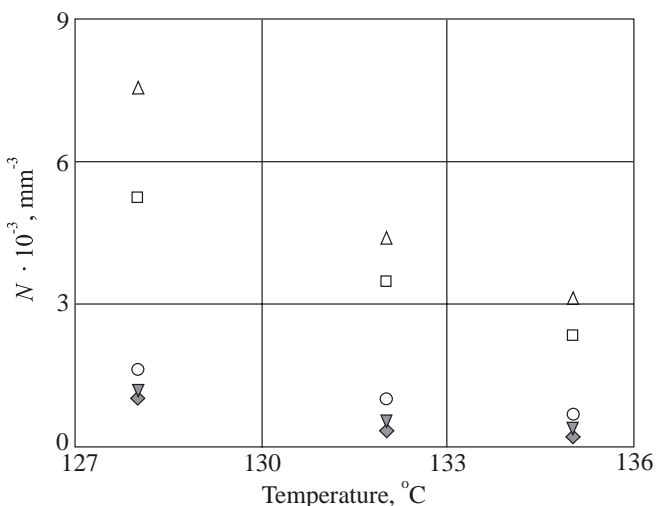


Fig. 8. Average number of spherulites per volume unit ( $N$ ) of DSC sample versus crystallization temperature for: compatibilized nanocomposites of polypropylene Malen P F401 with various MMT contents: (○) 3 wt. %, (□) 6 wt. %, (Δ) 10 wt. % and for blends of polypropylene Malen P F401 with various contents of the compatibilizer Polybond 3200: (◆) 20 wt. % and (▼) 33 wt. %

average spherulite numbers per volume unit found in neat Novolen *i*-PP's.

As it was demonstrated by the computer simulation of crystallization of nanocomposites, the value of  $R_s/R$  ratio used might lead to a certain overestimation rather than to underestimation of the average number of spherulites per volume unit. The numbers in Fig. 8 include also the spherulites nucleated at the late stage of crystallization in spite of the fact that they occupy only a small volume fraction of the sample. Based on the detailed studies of crystallization of the nanocomposites it was concluded in [9] that the late nucleation event is

related to the flow of a polymer melt towards crystallization front enforced by the density change and high sensitivity of the spherulite nucleation to the orientational flow in those nanocomposites. Thus, the nucleation effect of MMT in static conditions, at the beginning of crystallization, is even lower than that which follows from the data in Fig. 8.

## CONCLUSIONS

In order to calculate the correct average number of spherulites per unit volume of a sample the correct value of  $R_s/R$  ratio has to be used. As it was found by the computer simulation, this ratio depends on the mode of the nucleation process, which determines spherulite shapes and size distribution [14]. In the model case of nucleation occurring at a constant rate it is higher by 8 % (0.822 vs. 0.756) than in the case of instantaneous nucleation, which might introduce the error of 30 % in the estimation of  $N$  value. However, the dependence of the crystallization kinetics, and the average total number of spherulites in an area unit of a thin film on film thickness might introduce even higher error if not taken into account properly. On the contrary, if in addition to the instantaneous nucleation at the beginning of the crystallization, the second nucleation process occurs at the late stage of crystallization,  $R_s/R$  ratio may decrease by several percents from 0.756 to 0.704 (see the end of Computer Simulation Section).

As it follows from the derivations conducted in [12], ratios of characteristic distances in spherulitic structures are fully determined by the nucleation mode in the case of the nucleation either instantaneous or the nucleation at a rate proportional to the spherulite growth rate. Thus, the values of  $R_s/R$  ratios found by means of the computer simulation are valid independently on the intensity of the nucleation and on the spherulite growth rate.

The calculations of the nucleation density in the commercial grade polypropylene based on the proposed method were verified experimentally by the comparison with the results obtained by examination of thin films. The method was then applied to compare the nucleation density in polypropylenes differing in molecular weight. The most intense nucleation was found in polypropylene of the highest molecular weight.

The proposed method made also possible to determine the average number of spherulites in compatibilized polypropylene nanocomposites with montmorillonite and to understand better the nucleation effect of montmorillonite. Small spherulites nucleated in late stages of crystallization due to local polymer flow, although occupying only a small fraction of the sample volume might be numerous and influence significantly the average number of spherulites per volume unit calculated from the sections. The nucleation of spherulites caused by the presence of MMT at the beginning of the crystallization process in nanocomposites is rather weak

and we conclude that the nucleation in static conditions is at the level of the nucleation in neat commercial polypropylenes.

## REFERENCES

1. Hoffman J. D., Miller R. L.: *Polymer* 1997, **38**, 3151.
2. Avrami M.: *J. Chem. Phys.* 1939, **7**, 1103; *ibid.* 1940, **8**, 212; *ibid.* 1941, **9**, 177.
3. Ozawa T.: *Polymer* 1971, **12**, 150.
4. Grenier D., Prudhomme R. E.: *J. Polym. Sci., Polym. Phys. Ed.* 1980, **19**, 1655.
5. Piorkowska E., Galeski A.: *Polimery* 1994, **39**, 333.
6. Pakula T., Galeski A., Piorkowska E., Kryszewski M.: *Polym. Bull.* 1979, **1**, 275.
7. Billon N., Haudin J. M.: *Colloid Polym. Sci.* 1993, **271**, 343.
8. Galeski A., Piorkowska E.: *Polym. Bull.* 1980, **2**, 1.
9. Nowacki R., Monasse B., Piorkowska E., Galeski A., Haudin J. M.: *Polymer* 2004, **45**, 4877.
10. Galeski A.: *Polimery* 1978, **23**, 385.
11. Gadzinowska K., Piorkowska E.: *Polimery* 2003, **48**, 790.
12. Piorkowska E.: *J. Phys. Chem.* 1995, **99**, 14016; *ibid.* 1995, **99**, 14024.
13. Morawiec J., Pawlak A., Slouf M., Galeski A., Piorkowska E.: *Polimery* 2004, **49**, 52.
14. Galeski A., Piorkowska E.: *J. Polym. Sci., Polym. Phys. Ed.* 1981, **19**, 731.

Received 18 XII 2003.

### W kolejnym zeszycie ukaza się m.in. następujące artykuły:

- Nienasycone żywice poliestrowe w świetle wymagań Unii Europejskiej
- Synteza monomerów zawierających hydrofilowe ugrupowania sulfonianowe oraz wodorozcieńczalnych żywic poliestrowych na ich podstawie
- Synteza nienasyconych żywic poliestrowych w warunkach promieniowania mikrofalowego (*j. ang.*)
- Nienasycone żywice poliestrowe modyfikowane olejem roślinnym i dicyklopentadieniem
- Badania aktywności modyfikatorów aminowych z pierścieniem s-triazynowym w utwardzaniu nienasyconych żywic poliestrowych (*j. ang.*)
- Katalizatory syntezy żywic winyloestrowych z epoksynowolaku i nienasyconego kwasu monokarboksyłowego
- Modyfikacja powierzchni nienasyconych żywic poliestrowych za pomocą poli(perfluoroeterów) (*j. ang.*)
- Wpływ budowy chemicznej i struktury nadcząsteczkowej na właściwości mechaniczne kompozycji poliuretan/nienasycony poliester o wzajemnie przenikających się sieciach polimerowych
- Nanokompozyty nienasycony poliester/montmorylonit otrzymywane metodą interkalacyjnej poliaddycji *in situ* (*j. ang.*)
- Tiksotropowe kompozycje nienasyconych żywic poliestrowych z modyfikowanymi glinami smektycznymi
- Niektóre aspekty badań nad otrzymywaniem stałych termoutwardzalnych tłoczyw poliestrowych
- Rola różnych modyfikatorów w kompatybilizacji mieszanin PP/PET — charakterystyka reologiczna i strukturalna (*j. ang.*)
- Zastosowanie odpadowego fosfogipsu w kompozytach termoplastycznych i chemoutwardzalnych